Investigation of Various Laminating Materials for Interior Permanent Magnet Brushless DC Motor for Cooling Fan Application

A. Infantraj, M. Augustine, E. Fantin Irudaya Raj, and M. Appadurai

***Abstract*—Permanent magnet brushless DC motors are used for various low-power applications, namely domestic fans, washing machines, mixer grinders and cooling fan applications. This paper focuses on selecting the best laminating material for the interior permanent magnet brushless DC (IPM BLDC) motor used in the cooling fan of automobiles. Various laminating materials, namely M19-29GA, M800-65A and M43, are tested using finite element analysis. The machine's vital performance metrics, namely the stator current, torque ripple, and hysteresis loss were analyzed in selecting the laminating material. The designed motor is also modelled as a mathematical model from the computed lumped parameters. The performance of the machines was validated through electromagnetic and thermal analysis.**

***Index Terms*—Finite Element Analysis, IPM BLDC, Laminating Material, M19-29GA, M800-65A, M43.**

I. Introduction

MOSTLY, Permanent magnet (PM) motors suffer from a common problem called cogging torques. Carious cogging torque reduction strategies like skewing, pole pitch optimization, pole shape optimization, and usage of fractional slot/pole were proposed by [1]-[2]. A new stator and rotor pole design for BLDC motor to reduce torque fluctuation. The improved stator and rotor profiles have improved the air gap, thereby reducing the torque ripples [3]-[4]. A Neodymium free spoke-type BLDC motor was proposed to minimize the cost of the motor and maximize the torque by using ferrite magnets [5]. A reshaped rotor with modified symmetrical poles was proposed by [6], as modified asymmetrical poles and magnetic poles with grooves to reduce the cogging torque. A comparison between the outer rotor BLDC and BLAC motor to estimate the torque ripple using numerical analysis was proposed by [7].

Analytical procedures to design high-speed ferrite-based BLDC motors for electric vehicle applications to limit the demagnetization effects in permanent magnet rotors were proposed by [8]. A novel ferrite semi-modular dual stack BLDC motor for bore well application to reduce the flux leakage in the rotor without using a nonmagnetic hub was proposed by [9]. A comparative study on three types of ironless BLDC motor. Ironless BLDC motors have very little magnetic saturation, very less cogging torque and reluctance torque [10]. A modified stator tooth with T-shaped bifurcation was proposed by [11] for the reduction of cogging torque in BLDC motors.

A hybrid rotor made up of Neodymium and Ferrite permanent magnet was proposed to improve the output characteristics and reduce the effect of demagnetization by retaining the Torque per Rotor Volume (TRV) of neodymium permanent magnet motors [12]. Analysis of four different stator slot shapes was done by retaining the slot area and its performance on electromagnetic torque, efficiency, and flux density was assessed [13]. A two-dimensional (2D) analysis technique was proposed to make improvements in the stack length and thickness of PM in outer rotor BLDC motors [14]. The cogging torque reduction was achieved by implementing different skewed slot configurations for BLDC motors in small electric vehicle applications introduced [15]. To minimize the cogging torque in medium-powered PM motors, the rotor magnets of surface permanent magnet (SPM) are shifted, and its effect on variation in cogging torque was observed [16]. The stator dimensions, skewness, and magnet thickness were optimized for improved efficiency [17]-[18]. Various structural variations in the stator were made, and its influence on magnetic loading was observed [19].

The performance of the modified switched reluctance motor (SRM) in terms of torque density, torque ripple, and efficiency was investigated by implementing different laminating materials like M19, M850-65A, M890-50d, and M43 are compared with the conventional CR-10 steel material [20].

The influence of Sheet molding compound (SMC) material in the electrical drives enhances the performance by reducing the torque ripple. The analysis of SRM with different non-oriented steels has been explored [21]. The analysis of doubly salient permanent magnet SRM with different laminating materials has been illustrated [22]. The analysis of the literature reveals the importance of selecting the appropriate

Manuscript received February 16, 2023; revised May 15, 2023; accepted August 01, 2023. Date of publication December 25, 2023. Date of current version August 25, 2023.

A. Infantraj and M. Augustine are with Department of Electrical & Electronics Engineering, Loyola-ICAM College of Engineering & Technology, Chennai, Tamil Nadu, India (e-mail: infantt@gmail.com; gnanaugus@gmail.com).

E. Fantin Irudaya Raj is with Department of Electrical and Electronics Engineering, Dr. Sivanthi Aditanar College of Engineering, Tiruchendur, Tamil Nadu, India (e-mail: fantinraj@gmail.com).

M. Appadurai is with Department of Mechanical Engineering, Nehru College of Engineering and Research Centre, Thrissur, Kerala, India (e-mail: appadurai86@gmail.com).

(Corresponding Author: E. Fantin Irudaya Raj)

Digital Object Identifier 10.30941/CESTEMS.2023. 00048

laminating materials for the motor and motivates the analysis for segmented rotor SRM.

II. Motor Design and Modelling

Brushless permanent magnet DC motors are special electrical motors with a three-phase star/delta connected stator and permanent magnet rotor. The rotors are available in two structures, namely the surface permanent magnet (SPM) and interior permanent magnet (IPM) rotor. The interior permanent magnet offers better performance than SPM in terms of high torque density, greater speed range and better efficiency [23]-[24], making the motor most suitable for traction application. The IPM motors are available in various topologies, namely inset radial, IPM lateral, IPM curved, V-shaped and variable orientation. This paper focuses on the analysis of IPM radial inset topology.

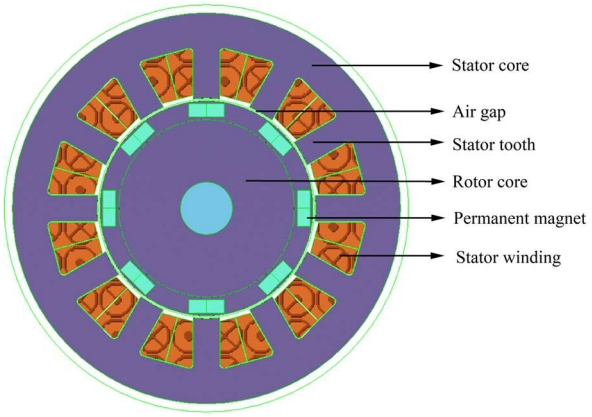

Fig. 1. 2D FEA Model of IPM BLDC Motor.

TABLE I
Dimensions of the IPM BLDC Motor

Specification	Dimension
Supply voltage in volts	12
Rated current in amps	40
Rated speed in revolution per minute	1000
Outer diameter in mm	74.9
Air gap thickness in mm	0.5
Stack height in mm	74.9
Rotor Inner diameter in mm	34
Rotor Outer diameter in mm	41.2
Magnet thickness in mm	2.5
Magnet width in mm	6.83
Stator Inner diameter in mm	42.2
Stator Outer diameter in mm	74.9

The proposed motor is designed based on the basic design equations [23] for 12 V and 500 W Cooling fan applications. The output power equation represented in equations (1) and (2) is used to determine the outer diameter and the stack length of the motor. The following parameters, namely the stator inner and outer diameter, rotor inner and outer diameter, the number of stator slots, the number of turns per phase, the number of rotor poles, length, and thickness of the magnet, are determined using the equations (3) to (9).is

$$Q = C_o D^2 L_{st} \times 10^{-3} \text{KVA} \tag{1}$$

$$C_o = 1.11\pi^2 k_m B_{\text{av}} ac \tag{2}$$

where,

Q – Output power in KVA.

C_o – Output coefficient.

D – Stator outer diameter in mm

L_{st} – Stack length in mm

B_{av} – Average flux density in Wb/m^2

ac – Specific electric loading.

k_m – Stacking factor.

The number of stator slots (S_s) is determined through

$$S_s = m \times p \times q \tag{3}$$

where,

m – Number of phases.

p – Number of rotor poles.

q – Integer.

The total air gap flux ($\varnothing_{tot}$) is given as

$$\varnothing_{tot} = B_{av} \times \pi DL \tag{4}$$

The emf(E_{ph}) is given as

$$E_{\text{ph}} = 4.44 \times f \times N_{\text{ph}} \times k_{\text{w}} \times \tag{5}$$

f – Frequency of the power supply in Hz.

N_{ph} – NNumber of turns per phase in the stator coil

k_{w} – Winding space factor.

$\varnothing_p$ – Flux per pole in weber.

Back emf (e)is given by

$$e = p\omega_m \frac{2N\varphi_g}{\pi} \tag{6}$$

where,

φ_g – Flux in the air gap.

ω_m – AAngular speed in rad/sec.

N – Total number of turns.

The electromagnetic torque (T) is given by.

$$T = 2NB_g L_{st} R_m i \tag{7}$$

where,

B_g – Air gap flux density.

R_m – RRadius of the rotor.

I – Stator current.

The air gap inductance (L_g)nd the flux concentration factor (C_φ)are calculated using the equations (8) and (9),

$$L_g = \frac{2\pi\mu_0 L_{st} R_m}{l_g + \frac{l_m}{\mu_r C_\varphi}} N^2 \tag{8}$$

$$C_\varphi = \frac{A_m}{A_g} \tag{9}$$

where,

μ_0 – Absolute Permeability of the free space.

μ_r – Relative permeability of the medium.

A_m, A_g is the area of magnet and airgap, respectively.

A 2D finite element methods (FEM) model is developed using Simcenter Magnet, as shown in Fig. 1. The design specification is mentioned in Table I. M19-29GA, M800-65A and M43 are used as the stator & rotor laminating material and

NdFeB is used as the permanent magnet material. The three-phase stator has four coils per phase, and each coil is wound with 17 turns per coil according to the layout represented in Table II.

TABLE II
WINDING LAYOUT OF IPM BLDC MOTOR

Phase	Coil No	Go	Return	No of Turns
Layout of phase A	1	1	2	17
	2	4	5	17
	3	7	8	17
	4	10	11	17
Layout of phase B	1	2	3	17
	2	6	6	17
	3	8	9	17
	4	11	12	17
Layout of phase C	1	3	4	17
	2	6	7	17
	3	9	10	17
	4	12	1	17

III. ELECTROMAGNETIC ANALYSIS

To analyze the operating performance of the proposed motor, 2D electromagnetic analysis is performed using Finite Element Analysis (FEA) tool. The material properties in terms of core loss coefficients are tabulated in Table III [20]. The rotor magnets are assigned with radially inward and outward permanent magnets. The motor is excited with a 12 V dc supply through a six-switch voltage source inverter. The flux lines of the permanent magnet and its interaction with the ac-excited stator are shown in Fig. 2. A maximum flux density of 2.5 Wb/m^2 is observed in the air gap during the interaction of flux between the stator and rotor. The leakage flux between the permanent magnet, stator back iron and the inner rotor are minimal. The simulation is run in constant velocity mode, and its variation on various performance metrics was observed by replacing the stator and rotor laminating materials.

TABLE III
CORE LOSS COEFFICIENTS FOR LAMINATING MATERIALS [20]

Laminating Material	Hysteresis Coefficient (W/kg)	Eddy current coefficient (W/kg)
M19-29GA	0.02703	0.5e-6
M43	0.0566	0.1e-6
M800-65A	0.0632	2.58e-5

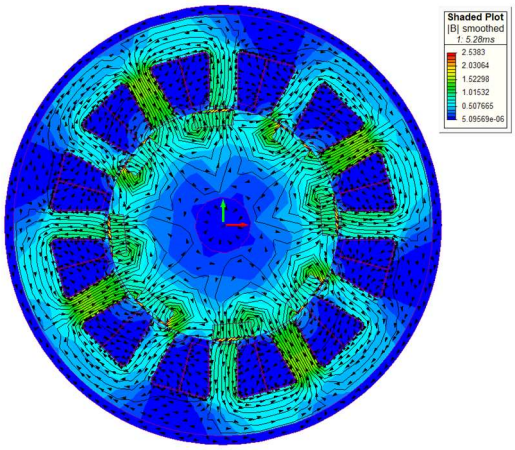

Fig. 2. Flux function of proposed SPM BLDC motor.

The performance parameters, namely the stator current, torque measured, and flux linkage of the proposed motor, are shown in Fig. 3 to 5, respectively. In terms of stator current, very less increment in current is observed for M800-65A over M43 and M19-29GA.

Similarly, the maximum torque observed for different materials is shown in Fig. 4. Not much improvement is observed in the flux linkage for the above-listed laminating materials.

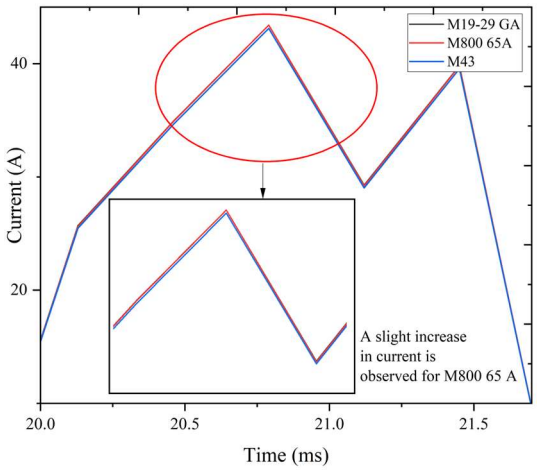

Fig. 3. Stator current waveforms of IPM BLDC.

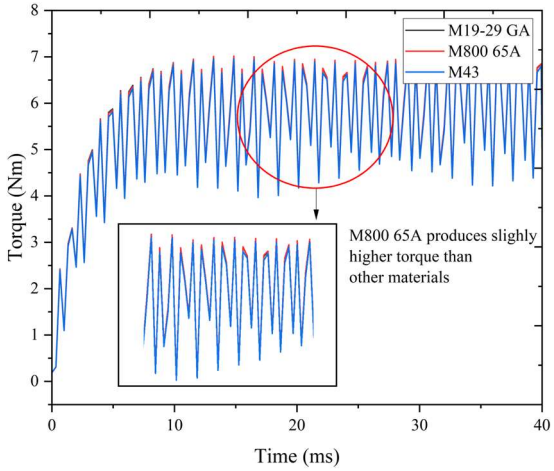

Fig. 4. Torque characteristics of IPM BLDC.

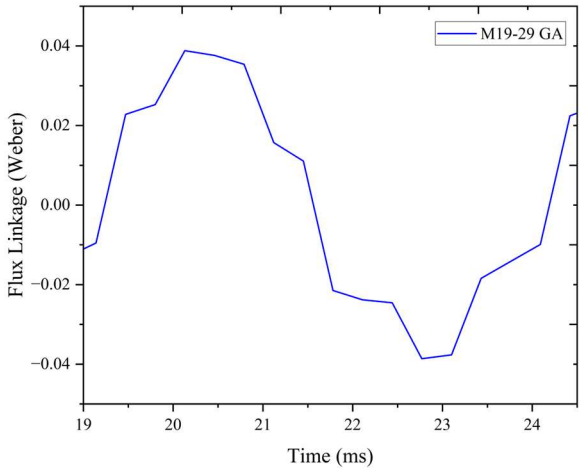

Fig. 5. Flux Linkage of IPM BLDC.

The proposed design exhibits trapezoidal flux, validating that this topology of the machine matches the typical flux pattern of BLDC motors. The change in the laminating material influences the performance efficiency of the IPM BLDC motor but does not provide any significant contribution to the torque ripple minimization, as reported in Table IV.

TABLE IV
PERFORMANCE COMPARISON

Laminating Material	Maximum Efficiency (%)	Torque Ripple (p.u)
M19-29GA	90.56	0.973
M43	90.4	0.973
M800-65A	85.49	0.973

IV. THERMAL MODEL

During electric motor running, the thermal energy is generated inside the stator slot, end windings, laminations, and rotor magnets because of the energy losses. Also, in special cases such as overload, and unsteady power conditions, the heat is generated enormously. This inducted heat is transferred throughout the electric motor components [25]. Proper disposal of heat is a crucial element while designing the electric motor. So, the generated waste heat inside the motor stator windings is transferred to air is a critical process that affects the performance and lifespan of the motor. Stator windings in electric motors generate heat due to electrical resistance during operation, and this heat must be dissipated to the surrounding air to prevent overheating and damage to the motor [26]. Overheating can lead to reduced performance, thermal stress, insulation breakdown, and, eventually, motor failure [27]. Effective heat transfer from the stator windings to air is important to ensure the reliability and longevity of the electric motor. The generated heat inside the stator winding is transferred to the air through two modes of heat transfer, namely conduction and convective type [28].

The rate of heat transfer from the stator to the atmosphere depends on several factors, namely the thermal conductivity of materials, surface area of the windings, temperature difference and surrounding air properties. The thermal conductivity and surface area of the windings are the constructional parameters which is modified on choosing the proper material [29]. Here, three different materials are chosen, and their heat transfer characteristics is studied using the finite element packages.

During the operation of the IPM BLDC motor, the magnetization and demagnetization cycle is made in the coil. Due to the various losses occurring in the motor, the losses are dissipated in the form of heat. The losses that occurred in the core of the IPM BLDC motor are estimated using the following equations (10) to (12),

$$P_{\text{core}} = P_{\text{hyl}} + P_{\text{edl}} \tag{10}$$

where,

P_{core} – Core loss.

P_{hyl} – Hysteresis loss.

P_{edl} – Eddy current loss.

$$P_{hyl} = k_h \times f \times B^{1.6} \times m \tag{11}$$

where,

k_h – Proportionality factor.

f – Frequency in Hertz.

B – Maximum value of magnetic flux density.

m – Mass of Iron core in kg.

$$P_{edl} = \left(\left(k_e (t \cdot f \cdot B)^2 \right) \Big/ \rho \right) \cdot m \tag{12}$$

where,

k_e – Proportionality Factor

t – Thickness of Laminated steel sheet

ρ – Resistivity of Laminated steel sheet

Fig. 6 and 7 illustrate the hysteresis losses and eddy current losses of the proposed motor with various laminating material. The hysteresis losses in the stator are higher than the rotor since this IPM BLDC motor has permanent magnet in the rotor and electromagnetic coil windings in the stator. When the stator is made of M43 materials, this type of loses is higher when compared to M800-65A and M19-29GA materials. The energy losses of amount 11 W are released while the stator is designed using M43 material.

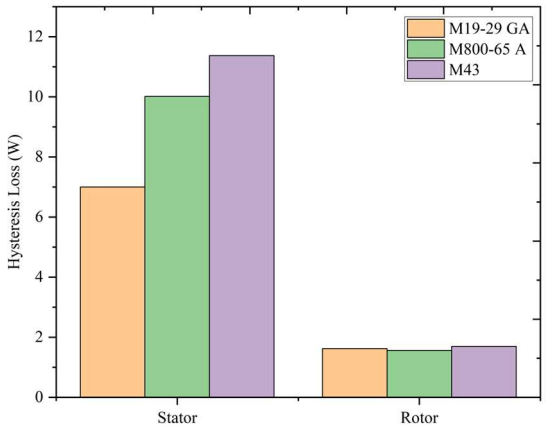

Fig. 6. Hysteresis Losses of various laminating material.

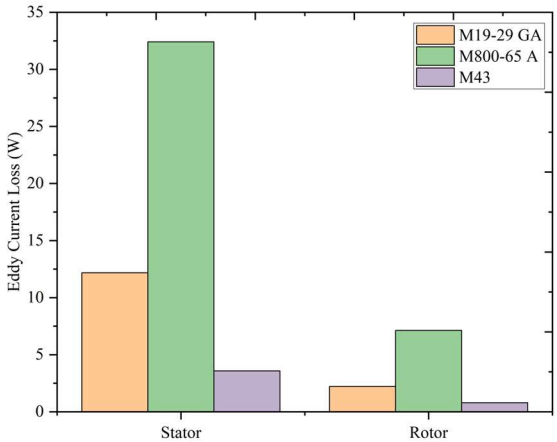

Fig. 7. Eddy current losses of various laminating material.

The interaction of variable magnetic field and conductor induces the eddy current in the electrical machines according to Faraday's law. This induced eddy current does not contribute any useful work in the motor and it is further considered as a loss. Sometimes it is labelled as an iron loss. While comparing the three stator materials, the M800-65A materials have a

higher eddy current loss of amount 32.5 W compared to the other two materials. The M43 materials have minimum eddy current losses while used in the stator and rotor designing. When comparing the stator and rotor altogether, the M19-29GA material yields better performance by means of minimum hysteresis losses and moderate eddy current losses.

Fig. 8-10 shows the temperature distribution of the stator and rotor components for different laminating materials. In this IPM-BLDC motor, the stator has copper coil winding, and the rotor has a permanent magnet. The heat is also transferred from the surface area of the coil windings to the atmospheric air through the convective mode of heat transfer.

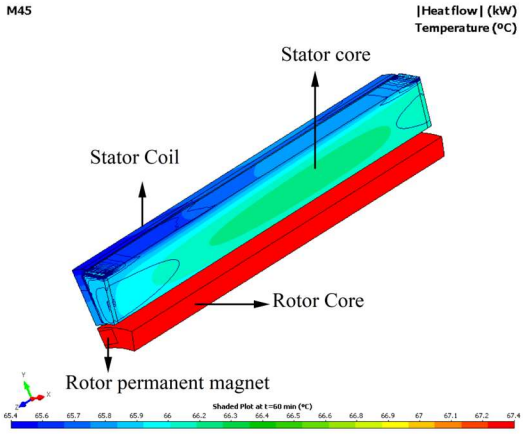

Fig. 8. Heat flow and temperature rise of M45.

In this present work, the numerical analysis is done for the IPM BLDC motor made of different materials in full-loaded conditions. The proposed motor is mainly used in automobile cooling fan applications. The aim of the cooling fan is to maintain the radiator coolant in the liquid phase. For this purpose, the proposed motor is supposed to be run on an intermittent duty cycle. Considering this motor operation, the simulations are also carried out in intermittent duty cycles. The energy losses from the coil winding are higher with respect to time during the starting conditions of the electric motor. This energy loss inducted the temperature in the electric motor parts. The temperature distribution around the electric motor stator and rotor components is obtained from the numerical analysis. From the temperature contour, the higher and lower temperature region is mentioned and identified.

The temperature distribution of the electric motor's stator and rotor component made of M45 material is shown in Fig. 8, M800-65A material is depicted in Fig. 9 and M19-29GA material is illustrated in Fig. 10. From the numerical analysis, it is found that the temperature is gradually rising with respect to time in transient conditions. Fig. 11 illustrates the temperature rise for 60 minutes duration for various materials in transient conditions. Initially, the temperature rise in the three materials is not much different. After a certain period, the temperature of the different materials is varied based on the physical characteristics of the materials. In these transient conditions, the temperature is increased gradually up to 55 minutes and becomes steady beyond this time. The temperature of the M800-65A materials is 67.8 °C at 55 minutes, which is the highest temperature attained in the numerical analysis. From this analysis, it is evident that the M19-29GA material yields better result and act as a better laminating material for the stator and rotor of the permanent magnet brushless DC motor.

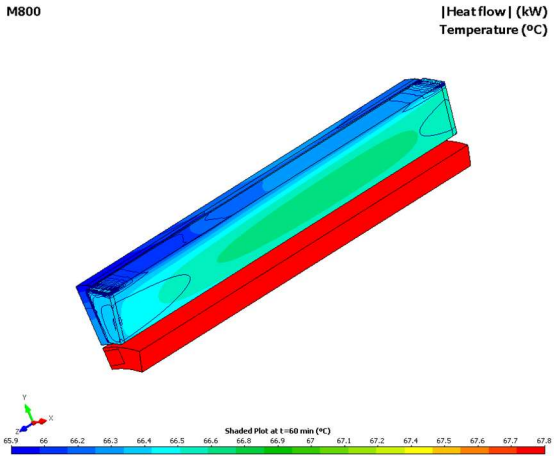

Fig. 9. Heat flow and temperature rise of M800-65A.

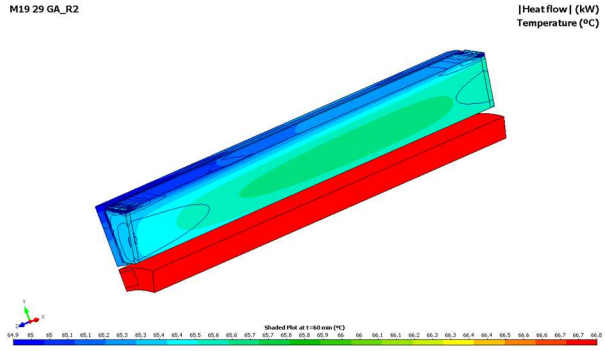

Fig. 10. Heat flow and temperature rise of M19-29 GA.

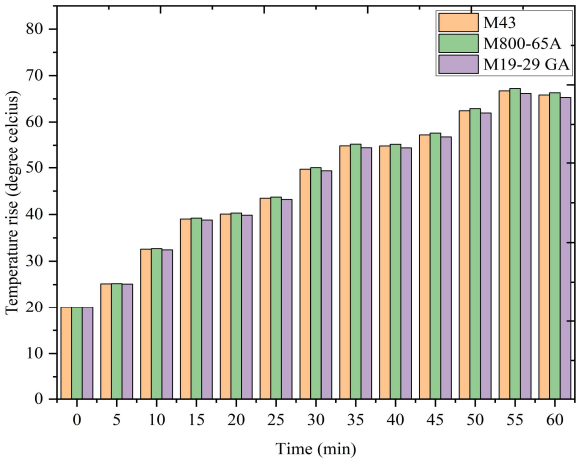

Fig. 11. Temperature rise for 60 minutes duration for various materials.

V. Electrical Equivalent Circuit Model

The lumped circuit parameters were estimated from the proposed 2D FEA model and an electrical equivalent circuit was modelled using SIMULINK [30] to test the motor for various operating conditions with a closed-loop electrical drive as shown in Fig. 12. The motor specifications are listed in Table V.

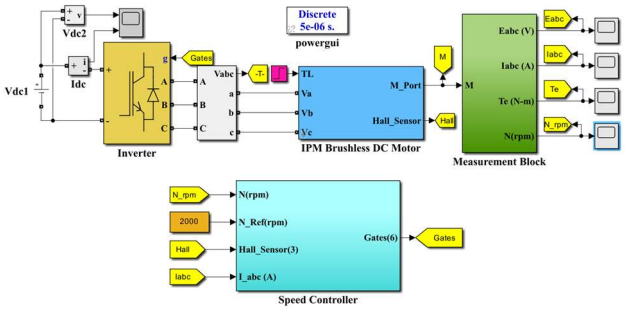

Fig. 12. Simulink model of IPM BLDC motor with closed loop control.

TABLE V
IPM BLDC MOTOR SPECIFICATION

Motor Parameters	Values
Rated voltage (V)	12
Back EMF constant Ke (V/(rad/s))	14.37
Torque constant Kt (N·m/A)	0.168
No-load speed (rpm)	3400
Stator phase resistance (ohm)	0.2455
Stator phase inductance (mH)	0.5277
RMS current (A)	7.0710

A conventional current controller with hysteresis control technique (HCC) [31]-[32] is implemented in this paper for testing the proposed IPM motor. The IPM motor is mathematically modelled using the phase voltage (V_a), back EMF (e) and electromagnetic torque (T) represented in equations (13) to (15),

$$V_a = RI_a + (L - M)\frac{d}{dt}(I_a) + e_a \tag{13}$$

where,

R – Stator phase resistance.

I_a – Phase current.

L – Self inductance.

M – Mutual inductance.

$$e = \frac{(\omega_m K_b f_{abc}(\theta))}{2} \tag{14}$$

where,

ω_m – AAngular speed.

K_b – Back EMF constant.

$f_{abc}(\theta)$ – Back EMF shaping function.

$$T = \frac{e_a I_a + e_b I_b + e_c I_c}{\omega_m} \tag{15}$$

where,

e_a, e_b, e_c, – Back EMF with respect to phases a, b, c, respectively.

I_a, I_b, I_c – Phase current with respect to phases a, b, c, respectively

The motor starts with no load, and a load torque of 1 Nm is applied after 0.8 ms. The stator currents exhibit a smooth flat-topped sine wave with a peak current value of 8 A, as shown in Fig. 13. The back EMF is modelled as a trapezoidal waveform through the shaping function. This shaping function is multiplied with speed and back EMF constant (K_e) to generate the back EMF signal. The K_e value is computed from the 2D FEA simulation. Ripples are observed in the flat portion of the back EMF waveform, as shown in Fig. 14, emulating the real-time characteristics of the permanent magnet motors.

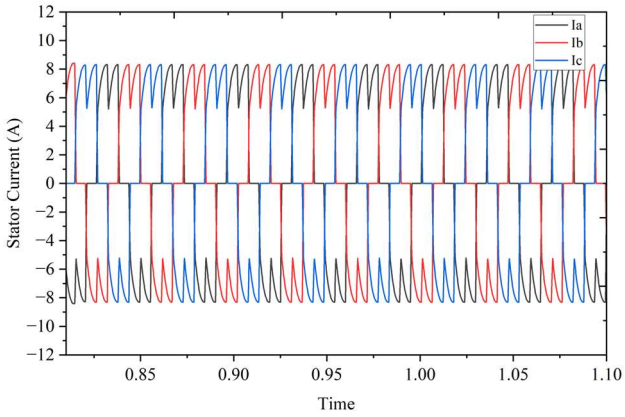

Fig. 13. Stator currents of IPM BLDC motor.

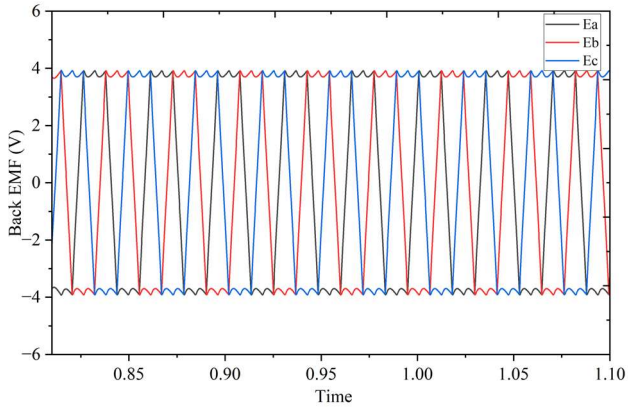

Fig. 14. Back EMF of IPM BLDC motor.

The motor starts with a starting torque of 0.8 Nm and reaches 7.1 Nm at 0.8 ms and with a torque ripple of 0.208 as shown in Fig. 15. The machine is simulated for a set speed of 2000 rpm and the closed loop controller attempts to reach the set speed after 1 ms as shown in Fig. 16.

VI. CONCLUSION

In this work, the IPM BLDC motor performance was investigated for an automotive cooling fan application. The fundamental design procedure was followed to design a 2D FEA motor model. The influence of laminating materials like

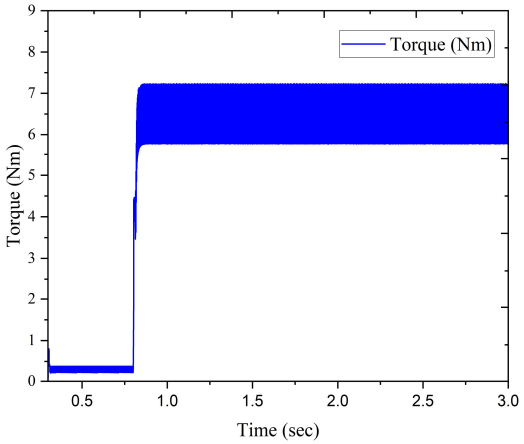

Fig. 15. Electromagnetic torque of IPM BLDC motor.

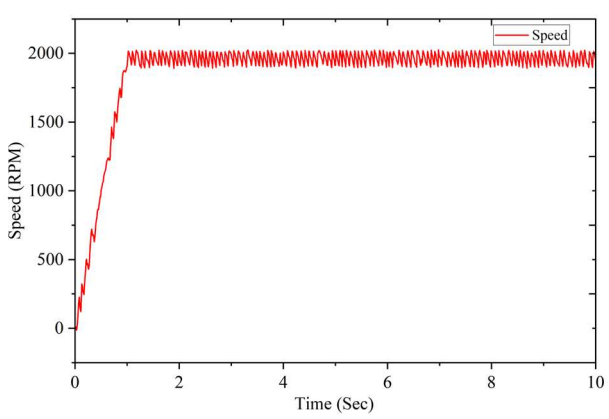

Fig. 16. Speed of IPM BLDC motor.

M19-29GA, M800-65A, and M43 on the proposed IPM BLDC motor was analyzed. The electromagnetic losses were fed as input to the thermal model as lumped parameters and the temperature rises for different lamenting materials were investigated. The temperature rise in the laminating material M19-29 GA is lesser than in other kinds of laminating material. To understand the behavior of control techniques used in the IPM BLDC motor, a dynamic simulation was carried out to implement the closed-loop speed control of the proposed motor. The result reveals better torque-speed characteristics for the given controller. Future work would be oriented towards the implementation of different control techniques to drive the proposed IPM BLDC motor and perform vibration analysis.

REFERENCES

[1] Z. Guo, L. Chang, and Y. Xue, "Cogging Torque of Permanent Magnet Electric Machines: an Overview," in *Proc. of 2009 Canadian Conference on Electrical and Computer Engineering*, pp. 1172-1177, St. John's, NL, Canada, May 2009.

[2] G. V. Ramana, T. V. Muni, and C. B. V. Subbarayud *et al*, "Improving the Maximum Power Point Tracking in Wind Farms with PID and Artificial Intelligence Controllers for Switched Reluctance Generators," in *Proc. of 2022 International Conference on Futuristic Technologies (INCOFT)*, Belgaum, India, Nov. 2022, pp. 1-6.

[3] S. K. Lee, G. H. Kang, and J. Hu *et al*, "Stator and Rotor Shape Designs of Interior Permanent Magnet Type Brushless DC Motor for Reducing Torque Fluctuation," *IEEE Trans. Magn.*, vol. 48, no. 11, pp. 4662-4665, 2012.

[4] E. Fantin Irudaya Raj, and M. Appadurai, "Minimization of Torque Ripple and Incremental of Power Factor in Switched Reluctance Motor Drive," in *Proc. of Recent Trends in Communication and Intelligent Systems: Proceedings of ICRTCIS 2020*, Singapore: Springer Singapore, 2021, pp. 125-133.

[5] H. C. Liu, H. W. Kim, and H. K. Jang *et al*, "Ferrite PM Optimization of SPM BLDC Motor for Oil-Pump Applications According to Magnetization Direction," *IEEE Trans. Appl. Supercond.*, vol. 30, no. 4, pp. 1-5, 2020.

[6] M. A. N. Doss, R. Sridhar, and M. Karthikeyan, "Cogging Torque Reduction in Brushless Dc Motor by Reshaping of Rotor Magnetic Poles with Grooving Techniques," *Int. J. Appl. Eng. Res.*, vol. 10, no. 36, pp. 27781-27785, 2015.

[7] T. Y. Lee, M. K. Seo, and Y. J. Ki *et al*, "Motor Design and Characteristics Comparison oof Outer-rotor-type BLDC Motor and BLAC Motor Based on Numerical Analysis," *IEEE Trans. Appl. Supercond.*, vol. 26, no. 4, pp. 1-6, 2016.

[8] A. Damiano, A. Floris, and G. Fois *et al*, "Design of a High-speed Ferrite-based Brushless DC Machine for Electric Vehicles," *IEEE Trans. Ind. Appl.*, vol. *53,* no. 5, pp. 4279-4287, 2017.

[9] S. Sashidhar, and B. G. Fernandes, "A Novel Ferrite SMDS Spoke-type BLDC Motor for PV Bore-well Submersible Water Pumps," *IEEE Trans. Ind. Electron.*, vol. 64, no. 1, pp. 104-114, 2016.

[10] L. Yang, J. Zhao, and X. Li *et al*, "Comparative Sudy of Three Different Radial Flux Ironless BLDC Motors," *IEEE Access*, vol. *6*, pp. 64970-64980, 2018.

[11] M. A. N. Doss, R. Brindha, and K. Mohanraj *et al*, "A Novel Method for Cogging Torque Reduction in Permanent Magnet Brushless DC Motor Using T-shaped Bifurcation in Stator Teeth," *Prog. Electromagn. Res. M*, vol. 66, pp. 99-107, 2018.

[12] C. L. Jeong, Y. K. Kim, and J. Hur, "Optimized Design of PMSM with Hybrid-type Permanent Magnet for Improving Performance and Reliability," *IEEE Trans. Ind. Appl.*, vol. *55,* no. 5, pp. 4692-4701, 2019.

[13] A. Kumar, R. Gandhi, and R. Wilson *et al*, "Analysis of Permanent Magnet BLDC Motor Design with Different Slot Type," in *Proc. of 2020 IEEE International Conference on Power Electronics, Smart Grid and Renewable Energy (PESGRE2020)*, Cochin, India, Jan. 2020, pp. 1-6.

[14] H. S. Shin, K. H. Shin, and G. H. Jang *et al*, "Experimental Verification and 2D Equivalent Analysis Techniques of BLDC Motor with Permanent Magnet Overhang and Housing-integrated Rotor Core," *IEEE Trans. Appl. Supercond.*, vol. 30, no. 4, pp. 1-5, 2020.

[15] V. Bogdan, M. Adrian, and L. Leonard *et al*, "Design and Optimization of a BLDC Motor for Small Power Vehicles," in *Proc. of 2021 International Conference on Electromechanical and Energy Systems (SIELMEN)*, pp. 438-443, Iasi, Romania, Oct. 2021.

[16] T. A. Anuja, and M. A. N. Doss, "Reduction of Cogging Torque in Surface Mounted Permanent Magnet Brushless DC Motor by Adapting Rotor Magnetic Displacement," *Energies*, vol. 14, no. 10, pp. 2861, 2021.

[17] O. Tosun, N. F. O. Serteller, and G. Yalcin, "Comprehensive Design and Optimization of Brushless Direct Current Motor for the Desired Operating Conditions," in *Proc. of 2021 25th International Conference Electronics,* Palanga, Lithuania, Jun. 2021, pp. 1-6.

[18] E. F. I. Raj, M. Appadurai, and E. F. I. Rani *et al*, "Finite-element Design and Analysis of Switched Reluctance Motor for Automobile Applications," *Multiscale and Multidisciplinary Modeling, Experiments and Design*, vol. 5, no. 3, pp. 269-277, 2022.

[19] A. Vadde, and S. Sachin, "Influence of Rotor Design in BLDC Motor for Two-wheeler Electric Vehicle," in *Proc. of 2021 1st International Conference on Power Electronics and Energy (ICPEE)*, Bhubaneswar, India, Jan. 2021, pp. 1-6.

[20] A. M. Gnaniah, B. Mahadevan, and K. Vijayarajan, "Influence of Laminating Materials and Modified Pole Shapes on the Performance of Segmented Rotor Switched Reluctance Motor," *Journal of Magnetics*, vol. 25, no. 3, pp. 347-354, 2020.

[21] H. Toda, K. Senda, and S. Morimoto *et al*, "Influence of Various Non-Oriented Electrical Steels on Motor Efficiency and Iron Loss in Switched Reluctance Motor," *IEEE Trans. Magn.*, vol. 49, no. 7, pp. 3850-3853, 2013.

[22] S. Prabhu, and M. Balaji, "Performance Analysis of Permanent Magnet Assisted Outer Rotor Switched Reluctance Motor with Non-oriented Laminating Material for Electric Transportation Systems," in *Proc. of 2022 IEEE 2nd International Conference on Sustainable Energy and Future Electric Transportation (SeFeT),* Hyderabad, India, Aug. 2022, pp. 1-6.

[23] J. R. Hendershot, and T. J. E. Miller, "*Design of brushless permanent-magnet machines,"* Venice, FL, USA: Motor Design Books, pp. 178, 2010.

[24] L. Balasubramanian, N. A. Bhuiyan, and A. Javied *et al*, "Design and Optimization of Interior Permanent Magnet (IPM) Motor for Electric Vehicle Applications," *CES Trans. Electr. Mach. Syst.*, vol. 7, no. 2, pp. 202-209, 2023.

[25] E. Fantin Irudaya Raj, and M. Balaji, "Analysis and Classification of Faults in Switched Reluctance Motors Using Deep Learning Neural Networks," *Arabian J. Sci. Eng.*, vol. 46, no. 2, pp. 1313-1332, 2021.

[26] D. V. Babu, K. Jyothi, and D. K. Mishra *et al*, "Visual Exploration of Fault Detection Using Machine Learning and Image Processing," *International Journal of Engineering Systems Modelling and Simulation*, vol. 14, no. 1, pp. 8-15, 2023.

[27] E. Fantin Irudaya Raj, and M. Appadurai, "Static 2D-Finite Element Analysis of Eccentricity Fault in Induction Motor," *Kolhe, M.L., Jaju, S.B., Diagavane, P.M. (eds) Smart Technologies for Energy, Environment*

and Sustainable Development, vol 1. Springer Proceedings in Energy. Springer, Singapore, 2022.

[28] E. F. I. Raj, M. Appadurai, and S. Darwin *et al*, "Detailed Study of Efficient Water Jacket Cooling System for Induction Motor Drive Used in Electric Vehicle," *International Journal on Interactive Design and Manufacturing (IJIDeM)*, pp. 1277–1288, 2023.

[29] M. Appadurai, E. F. I. Raj, and K. Venkadeshwaran, "Finite Element Design and Thermal Analysis of an Induction Motor Used for a Hydraulic Pumping System," *Mater. Today: Proc.*, vol. 45, pp. 7100-7106, 2021.

[30] A. C. Sijini, E. Fantin, and L. P. Ranjit, "Switched Reluctance Motor for Hybrid Electric Vehicle," *Middle East J. Sci. Res.*, vol. 24, no. 3, pp. 734-739, 2016.

[31] E. F. I. Raj, and V. Kamaraj, "Neural Network Based Control for Switched Reluctance Motor Drive," in *Proc. of 2013 IEEE International Conference on Emerging Trends in Computing, Communication and Nanotechnology (ICECCN),* Tirunelveli, India, Mar. 2013, pp. 678-682.

[32] M. Poovizhi, M. S. Kumaran, and P. Ragu *et al*, "Investigation of Mathematical Modelling of Brushless Dc Motor (BLDC) Drives by Using MATLAB-SIMULINK," in *Proc. of 2017 International Conference on Power and Embedded Drive Control (ICPEDC)*, Chennai, India, Mar. 2017, pp. 178-183.

A. Infantraj was born in Tamil Nadu, India, in the year 1985. He received the M.Tech degree in Applied Electronics from Karunya University, Coimbatore, India, in 2010. He is currently pursuing his Ph.D. in the Faculty of Information and Communication Engineering, at Anna University, Chennai, India.

He is currently working as an Assistant Professor in the Department of Electrical & Electronics Engineering, Loyola-ICAM College of Engineering & Technology, Chennai, India. His current research areas include electrical machine design, fault diagnosis of electric motors, solar and wind energy conversion systems, deep learning application in fault classification, fuel cells and embedded systems.

M. Augustine was born in Tamil Nadu, India in the year 1986. He completed his BE degree in Electrical and Electronics Engineering, ME degree in Power Electronics and Drives, and completed his Ph.D. degree from Anna University, Chennai.

He is working as an Assistant Professor at Loyola-ICAM College of Engineering and Technology, Chennai, Tamil Nadu, India, and has more than twelve years of teaching experience. He published papers in national and international journals. He is also acting as a reviewer for various international journals. His area of research includes Power Electronic Drives, Electrical Machines, and Embedded systems. He is an active professional member of ISTE and IAENG

E. Fantin Irudaya Raj was born in Tamil Nadu, India, in the year 1986. He completed his BE degree in Electrical and Electronics Engineering and ME degree in Power Electronics and Drives from Anna University, Chennai, in 2004 and 2011, respectively. Currently, he is pursuing his Ph.D. degree from Anna University.

Also, He was working as a part-time lecturer at the Government College of Engineering, Tirunelveli. He is currently working as an Assistant Professor at Dr. Sivanthi Aditanar College of Engineering, Tamil Nadu, India. He published more than 19 research articles in various international reputed journals. He participated in and presented his research ideas at more than 50 national and international conferences. He published one book in the engineering series and contribute numerous book chapters with various international recognized publishers. His area of research includes Electric motor drives, Renewable energy, Power Electronics, Image Processing, and Artificial Intelligence.

M. Appadurai was born in Tamil Nadu, India in the year 1986. He holds a B.E. degree in Mechanical Engineering from the Anna University, Chennai and a M.E. degree in Engineering Design from the Anna University, Tirunelveli and a Ph.D. degree in Mechanical Engineering from the Anna University, Chennai.

He worked as an Assistant Professor in the Department of Mechanical Engineering at Infant Jesus College of Engineering and Technology, Tamil Nadu for five years. He also worked as an Assistant Professor in the Department of Mechanical Engineering at Dr. Sivanthi Aditanar College of Engineering, Tamil Nadu for past ten years. He published several book chapters, books, conference papers and journals in the national and international level. He is presently working as an Associate Professor at Nehru College of Engineering and Research Centre, Kerala. He is an active professional member of ISTE and IAENG. His Professional interests include Solar Energy, Finite Element Analysis and Hybrid Electric Vehicles.